Toxicology and Applied Pharmacology 429 (2021) 115704

Contents lists available at ScienceDirect

Toxicology and Applied Pharmacology

journal homepage: www.elsevier.com/locate/taap

Selective antiproliferative effect of C-2 halogenated 13α-estrones on cells expressing Organic anion-transporting polypeptide 2B1 (OATP2B1)

Réka Laczkó-Rigó [a], Éva Bakos [a], Rebeka Jójárt [b], Csaba Tömböly [c], Erzsébet Mernyák [b], Csilla Özvegy-Laczka [a,*]

[a] Institute of Enzymology, Research Centre for Natural Sciences, Eötvös Loránd Research Center, Magyar tudósok körútja 2, H-1117 Budapest, Hungary
[b] Department of Organic Chemistry, University of Szeged, Dóm tér 8, H-6720 Szeged, Hungary
[c] Laboratory of Chemical Biology, Institute of Biochemistry, Biological Research Centre, Temesvári krt. 62, H-6726 Szeged, Hungary

ARTICLE INFO

Editor: Dr. Lawrence Lash

Keywords:
13α-estrones
Selective antiproliferative effect
Steroid uptake
OATP

ABSTRACT

Organic anion-transporting polypeptide 2B1 (OATP2B1) is a multispecific transporter mediating the cellular uptake of steroids and numerous drugs. OATP2B1 is abundantly expressed in the intestine and is also present in various tumors. Increased steroid hormone uptake by OATP2B1 has been suggested to promote progression of hormone dependent tumors. 13α-estrones are effective inhibitors of endogenous estrogen formation and are potential candidates to inhibit proliferation of hormone dependent cancers. Recently, we have identified a variety of 13α/β-estrone-based inhibitors of OATP2B1. However, the nature of this interaction, whether these inhibitors are potential transported substrates of OATP2B1 and hence may be enriched in OATP2B1-overexpressing cells, has not yet been investigated. In the current study we explored the antiproliferative effect of the most effective OATP2B1 inhibitor 13α/β-estrones in control and OATP2B1-overexpressing A431 carcinoma cells. We found an increased antiproliferative effect of 3-*O*-benzyl 13α/β-estrones in both mock transfected and OATP2B1-overexpressing cells. However, C-2 halogenated 13α-estrones had a selective OATP2B1-mediated cell growth inhibitory effect. In order to demonstrate that increased sensitization can be attributed to OATP2B1-mediated cellular uptake, tritium labeled 2-bromo-13α-estrone was synthesized for direct transport measurements. These experiments revealed increased accumulation of [^{3}H]2-bromo-13α-estrone due to OATP2B1 function. Our results indicate that C-2 halogenated 13α-estrones are good candidates in the design of anti-cancer drugs targeting OATP2B1.

1. Introduction

Organic anion-transporting polypeptides (OATPs) are membrane proteins mediating the cellular uptake of various endogenous and exogenous organic compounds in a Na^+ and ATP independent manner (Hagenbuch and Stieger, 2013). The known 11 human OATPs vary in their tissue distribution and substrate specificity. Some members of the OATP family are expressed ubiquitously in the human body (Konig et al., 2000; Roth et al., 2012), while others possess a tissue specific expression, like OATPs, 1B1 and 1B3, expressed exclusively in hepatocytes (Konig et al., 2000). OATPs, 1A2, 1B1, 1B3 and 2B1 are multispecific transporters recognizing a plethora of organic compounds, while for e.g., OATP1C1, a thyroid transporter, has a more limited substrate recognition pattern (Kovacsics et al., 2017; Pizzagalli et al., 2002) at least based on the available research data. Steroids, like bile acids and steroid hormones are common OATP substrates. OATPs, 1A2, 1B1, 2B1 and 4A1 are key participants in the cellular uptake of estrone-3-sulfate (E1S) and dehydroepiadrosterone-sulfate (DHEAS) and hence these OATPs are important in the maintenance of steroid hormone homeostasis (Rizner et al., 2017). On the other hand, altered expression of OATPs in tumors was documented by numerous studies (Buxhofer-Ausch et al., 2013; Thakkar et al., 2015). It has been proposed that elevated uptake of nutrients and hormones by OATPs provides a selective advantage of tumor cells over their healthy counterparts (Buxhofer-Ausch et al., 2013). For example, overexpression of OATPs, 1A2, 1B3 and 2B1 results in enhanced uptake of E1S and DHEAS and consequently issue in an increased survival of breast cancer cells in vitro (Arakawa et al., 2012; Matsumoto et al., 2015; Nozawa et al., 2004). Moreover, in

* Corresponding author.
E-mail addresses: rigo.reka@ttk.hu (R. Laczkó-Rigó), bakos.eva@ttk.hu (É. Bakos), tomboly.csaba@brc.hu (C. Tömböly), bobe@chem.u-szeged.hu (E. Mernyák), laczka.csilla@ttk.hu (C. Özvegy-Laczka).

https://doi.org/10.1016/j.taap.2021.115704
Received 24 April 2021; Received in revised form 6 August 2021; Accepted 26 August 2021
Available online 30 August 2021

vivo data from prostate cancer patients also underline that OATP expression promotes tumor progression. Enhanced testosterone uptake by OATP1B3, or DHEAS by OATP2B1 stimulates prostate cancer progression (Hamada et al., 2008; Wright et al., 2011). Therefore, inhibition of the uptake of hormones or hormone precursors by OATPs may be a potential strategy in the treatment of hormone dependent cancers.

On the other hand, multispecific OATPs also recognize various medicines, encompassing chemotherapeutics. Hence, they can potentially be targeted to increase intratumor accumulation of chemotherapeutic agents. For instance, OATPs, 1B1 and 1B3 transport atrasentan, sorafenib-glucuronide, SN-38 (the active metabolite of irinotecan), docetaxel, methotrexate, paclitaxel, and doxorubicin (Durmus et al., 2016). Additionally, OATP2B1, overexpressed in several cancers, including tumors of the breast, colon, bone and gliomas (Kovacsics et al., 2017), promotes the intracellular accumulation of abiraterone (Mostaghel et al., 2017), erlotinib (Bauer et al., 2018), etoposide (Fahrmayr et al., 2012), teniposide (Schafer et al., 2018) and SN-38 (Fujita et al., 2016). OATP2B1 has been shown to sensitize tumor cells to various chemotherapeutics (e.g.: tamoxifen, cytarabine) (Windt et al., 2019).

Inhibition of local estradiol synthesis through the inhibition of the aromatase or steroid-sulfatase (STS) pathways (e.g. by Exemestane or Irosustat, respectively (Gupta et al., 2013; Sang et al., 2018)) is a medical strategy to treat hormone dependent breast cancer in postmenopausal women. Recently, various 13α-estrone-derivatives have been developed that inhibit another key enzyme of local estradiol synthesis, 17β-hydroxysteroid dehydrogenase 1 (HSD1) (Ayan et al., 2011; Bacsa et al., 2015). 13α-estrone is the epimer of the natural 13ß-estrone that, due to a configurational change, cannot bind to the estrogen receptor and lacks hormonal activity (Ayan et al., 2011; Yaremenko and Khvat, 1994; Schonecker et al., 2000). Moreover, various 13α-estrones have been shown to inhibit the steroid transporter OATP2B1 as well (Jojart et al., 2018; Jójárt et al., 2021). Therefore, these derivatives are a promising novel, dual-target tool for the treatment of hormone sensitive cancers. Furthermore, if 13α-estrones were enriched in tumors by the function of OATP2B1 it could also potentially enhance their efficacy. Therefore, in the current study we investigated the antiproliferative effect of a set of previously identified 13α-estrone derivative OATP2B1 inhibitors to identify potential OATP2B1-transported substrates.

2. Materials and methods

2.1. Materials

If not stated otherwise materials were purchased from Sigma Aldrich, Merck (St. Louis, MO, US). The investigated steroids were synthetized as described elsewhere (Bacsa et al., 2018; Jojart et al., 2018; Jójárt et al., 2021).

Tritium labeling was carried out in a self-designed vacuum manifold (Schafer et al., 2015), radioactivity was measured with a Packard Tri-Carb 2100 TR liquid scintillation analyzer using Hionic-Fluor scintillation cocktail of PerkinElmer. Radio-HPLC was performed on a Jasco HPLC system equipped with a Packard Radiomatic 505 TR Flow Scintillation Analyzer.

2.2. Synthesis of 2-bromo-13α-estrone

2-Bromo- and 2,4-dibromo-13α-estrone were synthesized as described elsewhere (Bacsa et al., 2018).

2.3. Preparation of [^{3}H]2-bromo-13α-estrone ([^{3}H]2_2Br)

4.3 mg of 2,4-dibromo-13α-estrone (10 μmol) was dissolved in 0.6 mL of EtOAc in the presence of 5 mg of Pd/C (10% Pd) catalyst and 3 μL of triethylamine (21 μmol). The reaction mixture was degassed prior to tritium reduction by two freeze-thaw cycles, and then it was stirred under 0.18 bar of tritium gas for 2 h at rt. The excess tritium gas was then absorbed onto pyrophoric uranium and the catalyst was filtered off with a syringe filter. The filtrate was evaporated in vacuo and the labile tritium was removed by repeated evaporations from EtOH solution. Finally, 10.6 GBq of [^{3}H]13α-estrone (**2**) was isolated as a white solid that was immediately used for the next step. 450 MBq of [^{3}H]13α-estrone (**2**) was dissolved in 200 μL of dichloromethane and 28 μL of 1,3-dibromo-5,5-dimethylhydantoin dissolved in dichloromethane (5 mg/mL, 0.45 μmol) was added. The solution was stirred for 15 min then it was evaporated and the resulting solid was dissolved in tetrahydrofuran. HPLC purification resulted in 28 MBq of [^{3}H]**2_2Br**. The specific activity was determined by using an HPLC peak area calibration curve recorded with 2-bromo-13α-estrone (**2_2Br**) and it was found to be 555 MBq/mmol. The tritium labeled [^{3}H]2-bromo-13α-estrone ([^{3}H]**2_2Br**) was dissolved in EtOH (37 MBq/mL) and stored in liquid nitrogen.

2.4. Generation and maintenance of the cell lines

The A431 (human epidermoid carcinoma) cell line was purchased from ATCC. OATP2B1 and mock transfected A431 cell lines were generated as described previously (Patik et al., 2018). To generate cells with a fluorescent marker (green fluorescent protein, GFP or mCherry), A431 mock or A431-OATP2B1 cells were transduced with lentiviral supernatants produced with pRRL-EF1-mCherry or pRRL-EF1-eGFP expression plasmids (Windt et al., 2019). Cells were cultured in DMEM (Gibco, Thermo Fischer Scientific (Waltham, MA, US)) supplemented with 2 mM L-glutamine, 100 U/mL penicillin and 100 μg/mL streptomycin and 10% fetal calf serum at 37 °C with 5% CO_2 and 95% humidity.

2.5. Detection of OATP2B1 expression by Western blot

OATP2B1 expression in the cell lines was confirmed by Western blot as previously described in (Patik et al., 2018). Shortly, whole cell lysate of the OATP2B1 and mock transfected cell lines were separated on 7.5% SDS-PAGE gels and proteins were transferred onto PVDF membranes. The presence of OATP2B1 was detected by an anti-OATP2B1 antibody (a kind gift of Dr. Bruno Stieger, Department of Clinical Pharmacology and Toxicology, University Hospital, 8091 Zurich, Switzerland (Kullak-Ublick et al., 2001) with an epitope of: LLVSGPGKKPEDSRV). As a secondary antibody 20,000 × diluted HRP-conjugated anti-rabbit antibody (Jackson ImmunoResearch, Suffolk, UK) was used. Antibody raised against ß-actin was applied as an internal control (anti-ß-actin antibody (A1978, Sigma)) and in this case a HRP-conjugated anti-mouse secondary antibody was used (Jackson ImmunoResearch, Suffolk, UK) in 20,000 × dilution. Luminescence was detected by Luminor Enhancer Solution kit by Thermo Fisher Scientific (Waltham, MA, US).

2.6. Functional measurements

OATP2B1 expression was regularly checked by Zombie Violet (ZV, BioLegend®, San Diego, CA, US) uptake by flow cytometry (Patik et al., 2018). A431-OATP2B1 and mock transfected cells were collected after 0.1% trypsin treatment. The cells were washed with 1 mL uptake buffer (125 mM NaCl, 4.8 mM KCl, 1.2 mM $CaCl_2$, 1.2 mM KH_2PO_4, 12 mM $MgSO_4$, 25 mM MES, and 5.6 mM glucose, with the pH adjusted to 5.5 using 1 N NaOH). 5×10^5 cells were incubated with ZV (0.4 μL ZV/5×10^5 cells) for 15 min at 37 °C in a final volume of 100 μL. The reaction was stopped by adding 500 μL ice cold phosphate-buffered saline (PBS) and until the flow cytometry analysis the cells were kept on ice. The fluorescence of 10,000 living cells was determined by Attune NxT Flow Cytometer (Invitrogen, Carlsbad, CA).

2.7. Fluorescence-based measurement of cell proliferation

To measure the antiproliferative effect of the compounds, a fluorescence-based cell proliferation assay was performed as published in (Windt et al., 2019). The number of the fluorophore-labeled cells

(A431-mock-GFP and A431-OATP2B1-mCherry) is traceable over the incubation time, as the fluorescence is proportional with the number of the cells.

Cells were seeded in a density of 5×10^3 cells/well on 96-well plates in 100 μL in DMEM supplemented with 2 mM L-glutamine, 100 U/mL penicillin and 100 μg/mL streptomycin and 10% fetal calf serum. After 16–24 h the steroids diluted in 100 μL DMEM (0–50 or 0–100 μM final concentration) were added to the cells. As a control, 10 μM PZ-08 (3-*N*-benzyltriazolylmethyl-13α-estrone) was applied, previously shown to inhibit growth of A431 cells by 100% (Szabo et al., 2016b). The cells were cultured for 120 h at 37 °C with 5% CO_2 after which cellular fluorescence was recorded by a Perkin Elmer Enspire microplate reader (GFP: ex/em 485/510 nm; mCherry: ex/em 585/610 nm) by scanning the plate at a resolution of five points per well. Cell number was calculated based on the fluorescence values measured in non-treated (100%) or PZ-08-treated (0%) wells. Experiments were repeated in at least 3 biological replicates with 3 parallels in each. Mean ± SD values are shown.

2.8. Measurement of intracellular accumulation of 2_2Br

A431 mock control and A431-OATP2B1 cells (10^6 cells/sample) were incubated in the presence of 0.135 μM [^{3}H]**2_2Br** in a final concentration of 1 μM (or higher, see below) in 100 μL uptake buffer pH 5.5 for 10 min at 37 °C (or on ice, see Figure 8). The reaction was stopped by the addition of 1 mL ice-cold PBS and the cells were centrifuged at 300*g*. The cell pellet was collected in 100 μL PBS and pipetted into 1 mL Opti-Fluor (Perkin Elmer, Waltham, MA, US). Radioactivity was measured in a Wallac Liquid Scintillation Counter. Experiments were repeated three times.

Concentration dependent uptake was determined as described above with the exception that increasing concentrations of [^{3}H]**2_2Br** (1–100 μM) were applied for 5 min. For specific inhibition of OATP2B1, the cells were preincubated for 5 min in the presence of 20 μM bromosulfophtalein in uptake buffer pH 5.5. After 5 min 1 μM [^{3}H]**2_2Br** was added and the cells were further incubated for 10 min at 37 °C. Experiments were repeated in at least 3 biological replicates in which cells derived from different passages with 3 technical parallels.

2.9. Data analysis

All data are presented by calculating the mean ± SD obtained from at least three independent measurements, with 3 technical replicates in each individual experiment. The IC_{50} values were determined by sigmoidal curve fitting using the GraphPad Prism software (version 6 for Windows, GraphPad Software, San Diego, California, US). For statistical analyses unpaired Student's *t*-test was performed and the *p* value for statistical significance was set at $*p < 0.05$, $**p < 0.01$ or $***p < 0.001$, $****p < 0.0001$.

3. Results

3.1. Enhanced antiproliferative effect of 2-halogenated 13α-estrones on cells overexpressing OATP2B1

In our earlier studies we identified a series of 13α- and 13β-estrone derivatives that effectively inhibit the transport function of OATP2B1 (Jojart et al., 2018; Laczko-Rigo et al., 2020; Jójárt et al., 2021). However, the nature of these interactions, whether these compounds are inhibitors or substrates of OATP2B1 was not investigated. Therefore, in the current study estrones with high affinity to OATP2B1 ($IC_{50} \leq 2$ μM, see Figs. 1 and 2, and Table 1) were further investigated in an in vitro cell proliferation assay. In addition, as controls, in the case of halogenated 13α-estrones the less effective OATP2B1 inhibitor 4-C halogenated stereoisomers (**2_4** series, see Table 1) were also tested.

We hypothesized that transported toxic or cytostatic substrates of

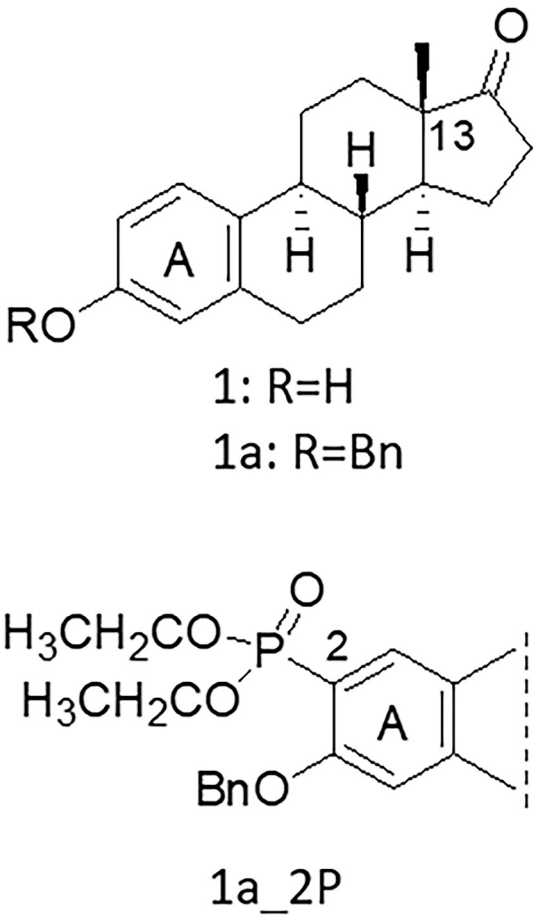

Fig. 1. Selected 13β-estrone-based high affinity OATP2B1 inhibitor (**1a_2P**).

OATP2B1, due to their increased uptake by OATP2B1, will result in increased antiproliferative effect in cells expressing OATP2B1 (Windt et al., 2019). For this aim, we used the A431 cell line overexpressing OATP2B1, generated earlier in our laboratory. A431-OATP2B1 is an ideal tool for microplate based functional measurements (Patik et al., 2018) including that of measuring cytotoxicity (Windt et al., 2019). In addition, it has been shown earlier that A431 cells are sensitive to certain 13α-estrone derivatives (Szabo et al., 2016b). In our study cell growth was followed by measuring the fluorescence of the protein used to tag the cells, GFP for mock transfected cells and mCherry for cells containing OATP2B1. We showed previously that fluorescence of GFP or mCherry is proportional to the cell number in the range of 5000–40,000 cells, and therefore this simple method can be used to monitor cell growth or death without the need of the addition of cell viability reagents (Windt et al., 2019). Expression and function of OATP2B1 was confirmed and regularly checked in the A431-OATP2B1-mCherry cell line (Fig. 3).

We found various degrees of cell proliferation inhibition of the OATP2B1 inhibitor 13α- and 13β-estrones. Estrone (**1**) had no significant antiproliferative effect on A431 cells, at least in the concentration range applied (Fig. 4). Similarly, 13α-estrone (**2**) and 3-*O*-methyl-13α-estrone (**2b**) had no effect on cell growth. However, 3-*O*-benzyl-13α-estrone (**2a**) exerted a well-measurable antiproliferative effect with an IC_{50} of 10.36 μM (Fig. 4 and Table 1).

We have demonstrated earlier that modification of the 13α- or 3β-estrone on C-2 or C-4 with diethylphosphite enhances its OATP2B1 inhibitory action (Jojart et al., 2018; Jójárt et al., 2021). Here we found that C-2 or C-4 diethylphosphonate modification of **2a** did not further increase cell growth inhibition as the IC_{50} values of 2- and 4- diethylphosphonates (15.91 μM and 10.52 μM, respectively) were unaltered

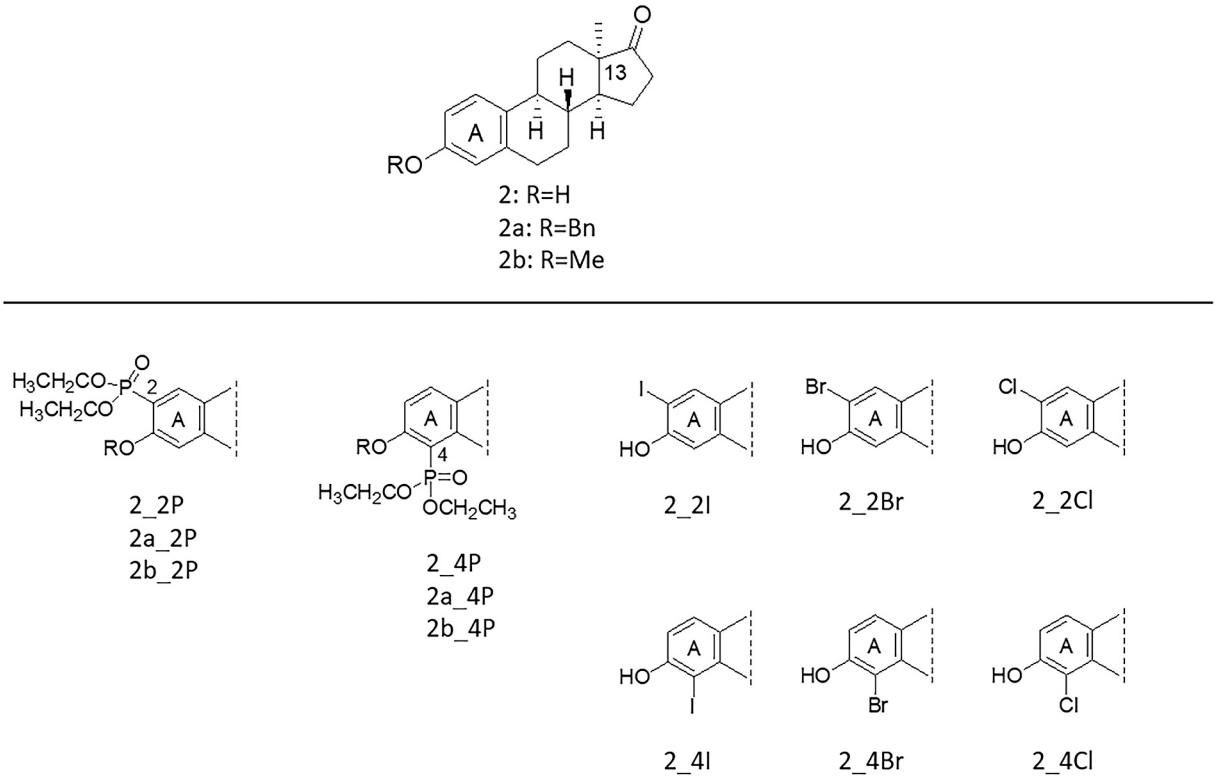

Fig. 2. Selected 13α-estrone-based high affinity OATP2B1 inhibitors.

Table 1
Inhibitory effect of the investigated compounds.

Name	IC_{50} ± *SD* (μM)	Name	IC_{50} ± *SD* (μM)
1	2.06 ± *0.043*	**2**[b]	>50
1a_2P[a]	0.041 ± *0.02*	**2_2P**[b]	2.8 ±*1.5*
2b[b]	3.4 ± *0.3*	**2_4P**[b]	1.4 ± *0.2*
2b_2P[b]	1.8 ± *0.3*	**2_2I**[c]	1.52 ±*0.01*
2b_4P[b]	2.8 ± *1.5*	**2_4I**[c]	6.63 ±*0.01*
2a[b]	1.7 ± *0.9*	**2_2Br**[c]	0.54 ±*0.02*
2a_2P[b]	0.2 ± *0.02*	**2_4Br**[c]	10.8 ±*0.02*
2a_4P[b]	0.3 ± *0.02*	**2_2Cl**[c]	2.11 ±*0.02*
		2_4Cl[c]	>50

Inhibitory effect of the compounds was described earlier, with the exception of compound **1**, a: (Jójárt et al., 2021), b: (Jojart et al., 2018), c: (Laczko-Rigo et al., 2020). Compounds were tested on A431-OATP2B1 cells in a transport assay using CascadeBlue hydrazide as test substrate. IC_{50} values were determined by nonlinear regression analysis fitted to the data points by GraphPad Prism software. Bold indicates compound names, italics is for SD values.

compared to **2a** (Figs. 4 and 5 and Table 2). Similarly, 2- and 4-diethylphosphonate variants of **2** (**2_2P** and **2_4P**) and the 2- diethylphosphonated version of 3-*O*-methyl-13α-estrone (**2b_2P**) were found to have no major effect on cell growth.

On the other hand, 3-*O*-benzyl-13α- and 13ß-derivatives (**2a** series and **1a_2P**) resulted in significantly increased cell growth inhibition with IC_{50} values of around 10 μM (Fig. 5 and Table 2). However, in spite of their high affinity inhibition of OATP2B1 function, none of these compounds showed increased cell growth inhibition in A431-OATP2B1 cells as compared to the mock-transfected controls.

Similarly to the diethylphosphonated derivatives, the halogen substituted derivatives of **2** (**2_2I, 2_2Br, 2_2Cl, 2_4Br or 2_4Cl**) had no or only marginal (**2_2I or 2_4I**) effect on mock-transfected cells. However, the C-2 halogenated compounds showed increased cell growth inhibition (see Fig. 6 and Table 2) in cells overexpressing OATP2B1. The selective cell growth inhibition of C-2 halogenated 13α-estrones in OATP2B1-overexpressing cells can be interpreted as the result of cellular enrichment of these compounds by OATP2B1. Indeed, we found that inhibiting OATP2B1 function with the OATP-specific inhibitor bromosulfophthalein (BSP) could partially block the effect of 2_2Br in A431-OATP2B1 cells (Supplementary Fig. S2A).

3.2. Synthesis and tritium labeling of 2_2Br

In order to investigate the possible OATP2B1-mediated transport of the most selective compound (with a 4-fold selectivity ratio, Table 2), radioactive labeling of 2-bromo-13α-estrone (**2_2Br**) was performed. Tritium labeling was carried out by catalytic dehalogenation of the *bis*-brominated compound 2,4-dibromo-13α-estrone in the presence of tritium gas followed by mono-bromination of [^{3}H]**1** at the C-2 position. The regioselective bromination cannot be achieved under various conditions, and thus, a mixture of brominated compounds was obtained. Next, an HPLC method was developed for the separation of the compounds [^{3}H]**2_2Br**, [^{3}H]**2_4Br** and the *bis*-brominated **2_2/4Br**. The bromination of [^{3}H]**1** was performed in the presence of DDH with an optimal yield of [^{3}H]**2_2Br** that was isolated by HPLC separation (Supplementary Fig. S1).

3.3. OATP2B1-mediated accumulation of [^{3}H]-2-bromo-13α-estrone ([^{3}H]2_2Br)

Cellular accumulation of [^{3}H]**2_2Br** was measured in A431-OATP2B1 and mock control cells. We found that OATP2B1-overexpressing A431 cells accumulated twice more [^{3}H]**2_2Br** than

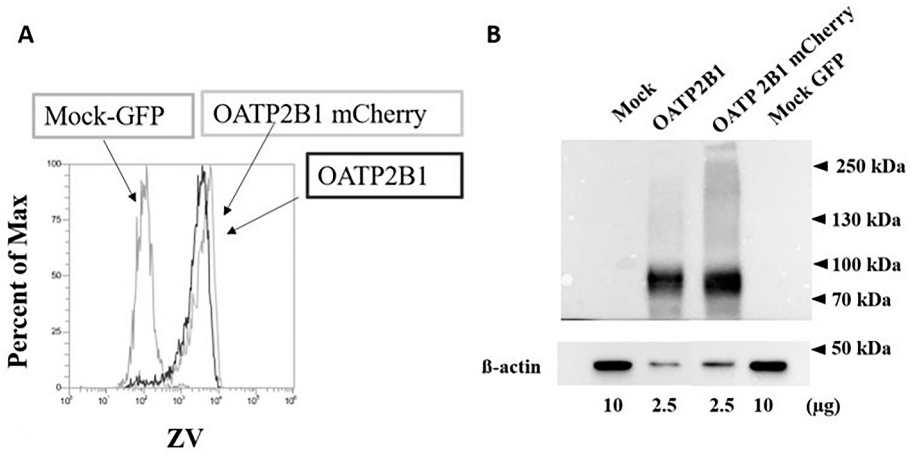

Fig. 3. A. Zombie Violet uptake in OATP2B1 and mock transfected cells. The histogram shows the uptake of the Zombie Violet (ZV, 250x diluted) fluorescent dye, a known substrate of OATP2B1 (Patik et al., 2018). A431 cells were incubated for 15 min at 37 °C in uptake buffer (pH 5.5). Fluorescence was monitored by flow cytometry. Experiments were repeated every week in order to control OATP2B1 expression. A representative histogram is shown. B. Expression of OATP2B1 in A431 cells confirmed by Western blot. OATP2B1 was detected by an anti-OATP2B1 antibody (Kullak-Ublick et al., 2001) and ß-actin was used as loading control. Experiments were repeated at least three times. One representative blot is shown.

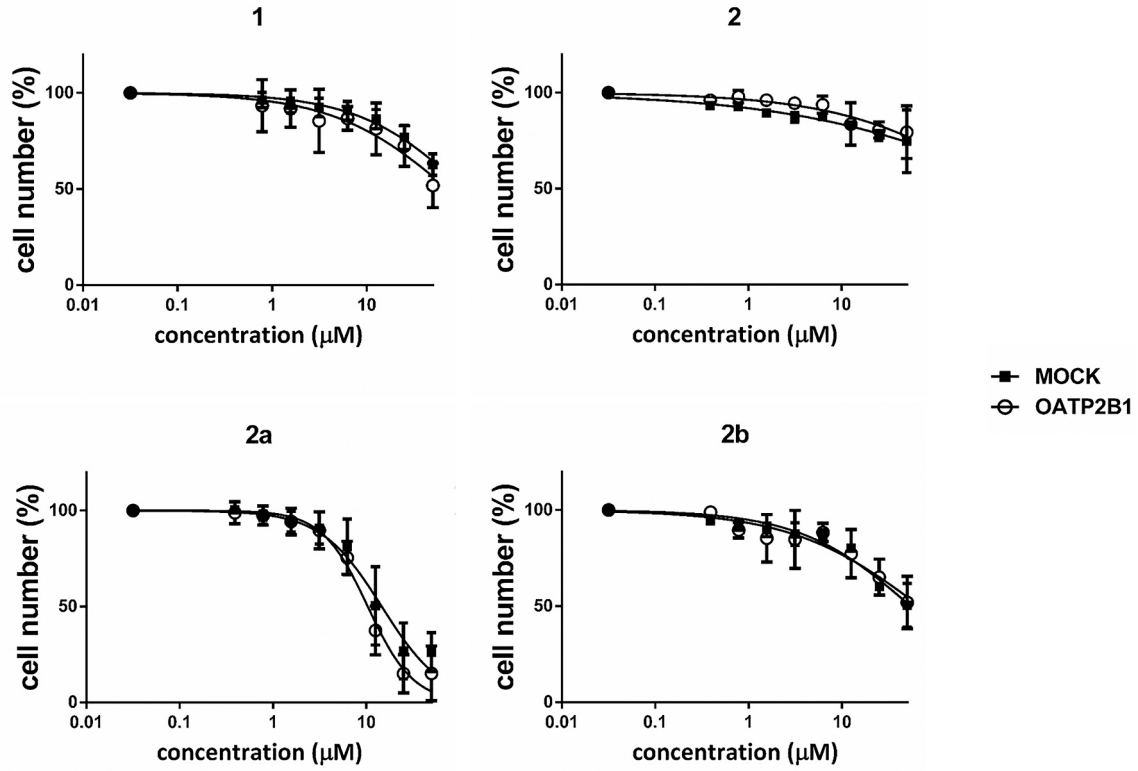

Fig. 4. Cell growth inhibition of compounds in A431 cells. A431 mock and A431-OATP2B1 cells were incubated with increasing steroid concentrations for 120 h on 96-well plates. Cell number was determined based on the fluorescence of mCherry or GFP measured in an Enspire fluorescence plate reader, 100%: in the absence of estrones. Data show the mean ± SD values obtained from at least three independent measurements.

the control A431 cells (Fig. 8A). The concentration dependence of the cellular uptake of **[^{3}H] 2_2Br** in the range of 1–100 µM (at both pH 5.5 (Fig. 8B) and pH 7.4 (Supplementary Fig. S3)) indicated a transporter mediated uptake mechanism that was further confirmed by the significantly decreased transport in the presence of the OATP-specific inhibitor bromosulfophthalein, and by the lack of transport at 4 °C (Fig. 8C).

4. Discussion

OATP2B1 is a plasma membrane protein mediating intestinal and hepatic uptake of its substrates. On the other hand, OATP2B1 is also overexpressed in tumors of the colon, bone, breasts and gliomas (Kovacsics et al., 2017). Since OATP2B1 is a multispecific transporter recognizing a large set of chemically diverse compounds, including various drugs, one anti-tumor strategy could be to exploit its activity to increase intra-tumor concentrations of its substrate chemotherapeutics. Indeed, we have recently shown that OATP2B1 can sensitize the cells toward chemotherapeutics (Windt et al., 2019).

Synthetic steroids, e.g. the estrogen receptor degrader Fulvestrant (Lee et al., 2017) and the aromatase inhibitor Exemestane (Van Asten et al., 2014) are frequently administered for hormone receptor positive breast cancers. However, steroid-based compounds face the challenge of lacking estrogenic activity. 13α-estrone derivatives are good candidates for anticancer treatment, since they have no hormonal activity, but interfere with local estrogen synthesis by inhibiting the STS and/or HSD1 enzymes. Indeed, several 13α-estrone derivatives were identified as antiproliferative agents against various cancer cell lines (Berenyi et al., 2013; Szabo et al., 2016a). However, for example, 3-benzyl ether

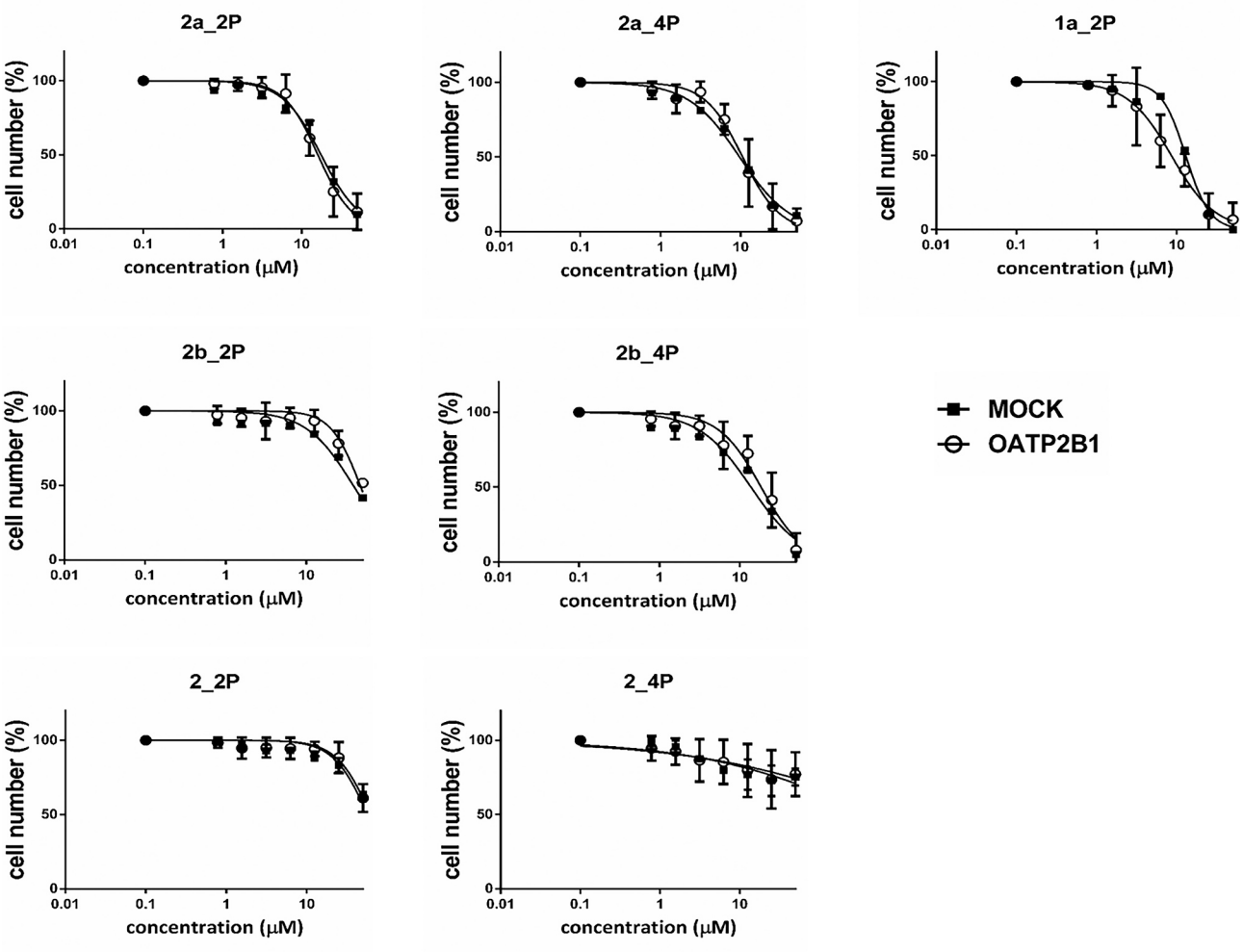

Fig. 5. Effect of C-2 or C-4 diethylphosphonated 13α-estrone derivatives on the proliferation of A431 cells. A431 mock and A431-OATP2B1 cells were incubated with increasing steroid concentrations for 120 h. Cell number was determined based on mCherry or GFP fluorescence measured in an Enspire plate reader. Data show the mean values ± SD calculated from at least three independent measurements.

Table 2
Antiproliferative effect of the compounds on OATP2B1 and mock transfected cells.

Name	IC_{50} ± *SD* (μM)		Name	IC_{50} ± *SD* (μM)		SR
	2B1	mock		2B1	mock	
1	42.01 *±0.033*	36.36 *±0.029*	**2**	>50	>50	
1a_2P	8.552 *±0.05*	12.89 *±0.027*	**2_2P**	>50	>50	
2b	>50	>50	**2_4P**	>50	>50	
2b_2P	46.42 *±0.022*	38.03 *±0.028*	**2_2I**	**15.78** *±0.051*	**36.57** *±0.016*	2.32****
2b_4P	18.32 *±0.036*	13.71 *±0.036*	**2_4I**	27.76 *±0.022*	28.48 *±0.167*	1.03
2a	10.36 *±0.03*	14.65 *±0.042*	**2_2Br**	**32.4** *±0.017*	**129.8**^{x} *±0.056*	4.01****
2a_2P	15.91 *±0.03*	17.45 *±0.039*	**2_4Br**	77.52^{x} *±0.051*	95.83^{x} *±0.084*	1.24
2a_4P	10.52 *±0.036*	9.67 *±0.038*	**2_2Cl**	**23.92** *±0.014*	**51.21** *±0.013*	2.14*
			2_4Cl	67.01 *±0.024*	251.8^{x} *±0.037*	3.75

IC_{50} values were determined by nonlinear regression analysis fitted to the data points by GraphPad Prism software. SR = selectivity ratio: IC_{50} in mock/IC_{50} in OATP2B1, ^{x}: data were predicted by GraphPad Prism software. Statistically significant difference between IC_{50} values: *$p < 0.05$, ****$p < 0.0001$. Bold indicates compound names, italics is for SD values.

of the 16-oxime propionate in the 13α-estrone series was shown to be toxic not only to HeLa and MCF-7 cells, but also to A431 cells lacking the STS and HSD1 enzymes (Szabo et al., 2016a). In addition, triazolyl-13α-D-secoestrone derivatives exerted an excellent antiproliferative potential on human cervical (HeLa, C33), ovarian (A2780) and HR^{+} breast (MCF-7, T47D) cancer cell lines (Berenyi et al., 2013).

Previously, we have shown that 13α- or 13β-estrone derivatives, originally designed to inhibit the STS and HSD1 enzymes, are effective inhibitors of OATP2B1 function (Jojart et al., 2018; Laczko-Rigo et al., 2020; Jójárt et al., 2021). Hence, these estrones can be good candidate dual-targeted molecules simultaneously aiming a tumoric transporter as well as an enzyme. We hypothesized that if transported by OATP2B1 these compounds can be enriched in and be more toxic to the cells overexpressing the transporter. Hence, we further investigated a set of these OATP2B1 inhibitor 13α-estrones (Fig. 2) and a recently identified OATP2B1 inhibitor with a nanomolar inhibitory constant, phosphonated 13β-estrone (**1a_2P**, Fig. 1) (Jójárt et al., 2021), for their ability to inhibit the proliferation of OATP2B1-overexpressing cells. For this aim, the A431 cell line, a well-established model for the investigation of OATP function (Windt et al., 2019) was applied. Although the toxicity of 13α-estrones in A431 cells has not yet been investigated in detail, various 13α-estrones have been shown to be toxic in A431 cells (Szabo et al., 2016b).

From the set of the investigated compounds, we found that 3-*O*-benzyl derivatives (**2a**, **2a_2P**, **2a_4P**, **1a_2P** and **2a_4P**) had increased

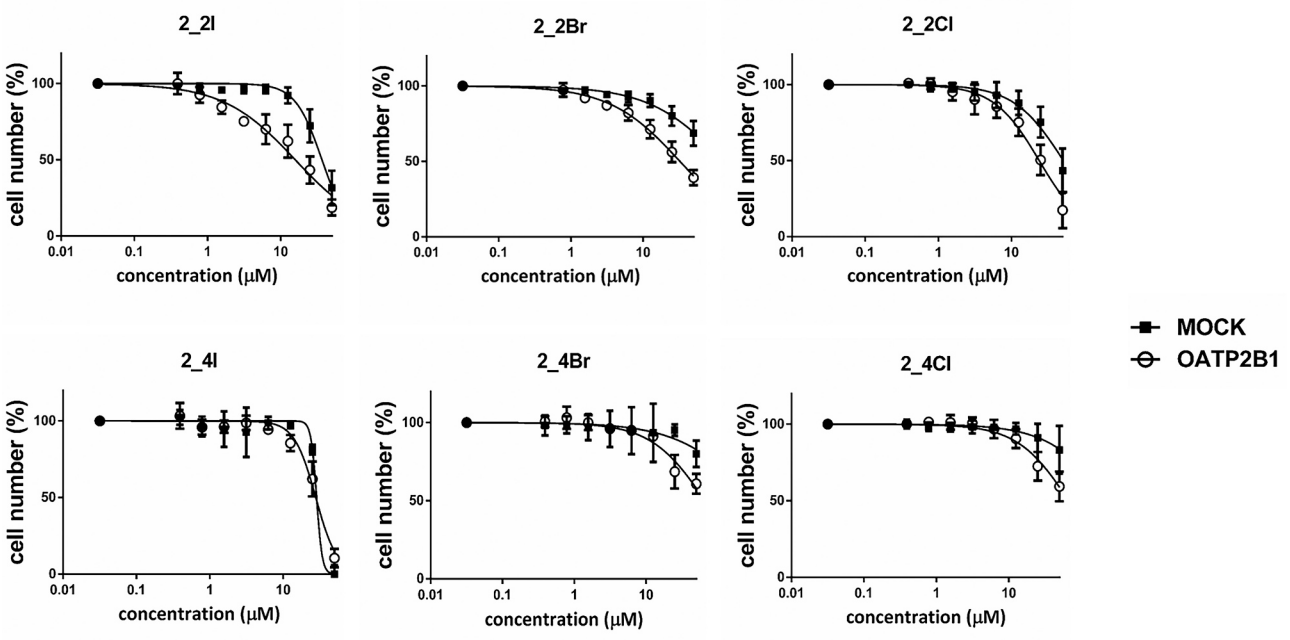

Fig. 6. Effect of C-2 or C-4 halogenated 13α-estrone derivatives on growth of A431 cells. A431 mock and A431-OATP2B1 cells were incubated with increasing steroid concentrations for 120 h on 96-well plates. Cell number was determined based on the fluorescence of mCherry or GFP in an Enpsire fluorescence plate reader. Data show the mean ± SD values obtained from at least three independent measurements.

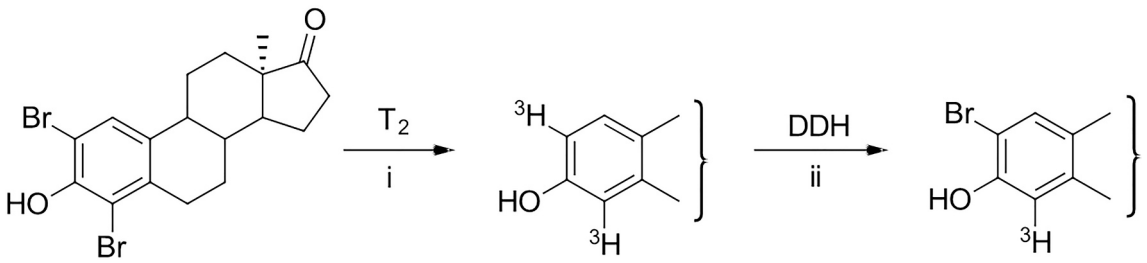

Fig. 7. Tritium labeling of **2_2Br.** (i) Pd/C (10% Pd), $^3H_2$, EtOAc, TEA; (ii) 1.2 equiv. DDH, CH_2Cl_2, 15 min, rt.

antiproliferative effect on A431 cells (their IC_{50} values below 20 μM) irrespective of the presence of OATP2B1. This harmonizes with our previous findings, various 13α-estrones with a C-3 *N*-benzyl-triazolylmethoxy moiety being toxic on A431 cells (Szabo et al., 2016b). In the current study C-2 or C-4 iodinated 13α-estrones also resulted in a moderately increased antiproliferative effect (IC_{50} values around 30 μM) compared to the core 13α-estrone. While here only a limited set of compounds was investigated, since our study focused on the highest affinity inhibitors of OATP2B1 function, we observed that the introduction of a large substituent on 3-hydroxy function of the initial compounds 13α- or 13β-estrone issued in enhanced cell growth inhibition effect.

The OATP2B1-selective antiproliferative effect was observed exclusively in the case of the 2-halogenated compounds. **2_2I**, **2_2Br** and **2_2Cl** resulted in a 2-, 4- and 2-fold decreased IC_{50} in A431-OATP2B1 cells, respectively (Fig. 6 and Table 1). The C-4 halogenated counterparts were less effective inhibitors of OATP2B1 function, accordingly, they did not result in an OATP2B1-selective anti-proliferative effect. Furthermore, the OATP2B1-selective antiproliferative effect of **2_2Br** could be inhibited by bromosulfophthalein (Supplementary Fig. S2A). In further experiments we demonstrated the OATP2B1-mediated uptake of the most selective compound **2_2Br** (Fig. 8) that may explain its enhanced antiproliferative effect in OATP2B1-overexpressing cells.

The 13α-estrones investigated here have been designed to inhibit the HSD1 enzyme (Bacsa et al., 2015; Jojart et al., 2018), and hence decrease the proliferation of hormone dependent tumors. A431 cells lack HSD1 and are hormone independent, however they are enriched in the 17ß-HSD type 2 (HSD2) enzyme (Blomquist et al., 1997). HSD2 has been shown to be inhibited by C18, C19 and C21 steroids (Blomquist et al., 1984), therefore, the investigated steroids may act through the inhibition of HSD2 in A431 cells. On the other hand, increased expression of estrogen-related receptor alpha (ERRα) has been documented in A431 cells (Chen et al., 2018). ERRα is an orphan nuclear receptor, of which upregulation is involved in the development of estrogen-independent tumors (Chen et al., 2018). Accordingly, suppression of ERRα inhibited A431 cell proliferation (Chen et al., 2018). However, whether the antiproliferative effect of 13α-estrones observed in our study can be related to the inhibition of the ERRα receptor needs further investigations. Interestingly, **2_2Br** had only a slightly increased antiproliferative effect in estrogen-dependent T47D breast cancer cells (also expressing the HSD1 enzyme, Supplementary Fig. S2B) indicating that the compound may exert its antiproliferative effect independent of the estrogen pathway. Recently, 13α-estrones have been described as inhibitors of tubulin formation (Jojart et al., 2020), therefore this can be an alternative mechanism of cell growth inhibition in A431 cells.

Many illnesses including cancer treatment require the simultaneous action on multiple targets in order to avoid drug resistance mechanisms, to increase effectiveness and to prolong overall survival. This is often achieved by drug “cocktails”. However, by the application of “cocktail therapy” the incidence of drug-drug interactions and off-target effects

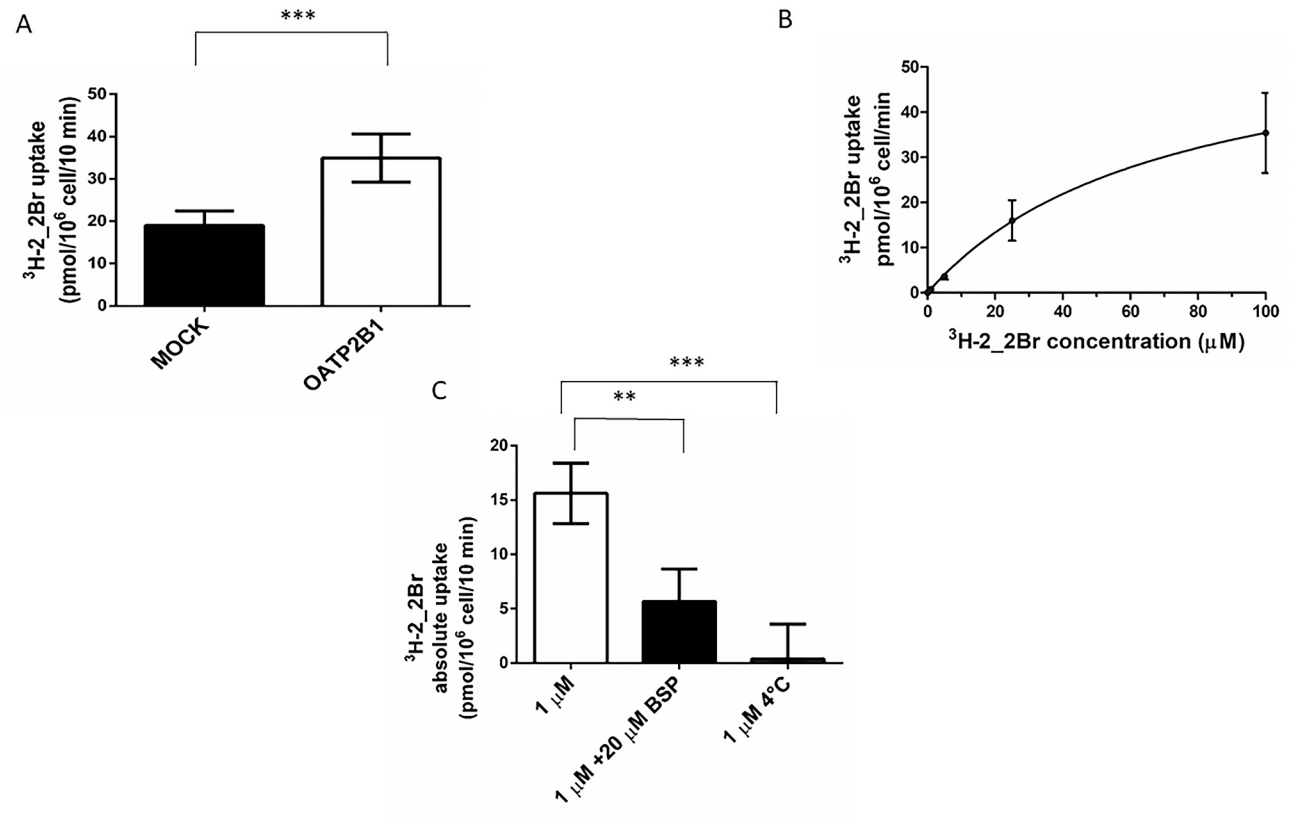

Fig. 8. A. Uptake of **[^{3}H] 2_2Br** in A431 cells. A431-OATP2B1 cells and their mock transfected counterparts were incubated with 1 μM (A) or 1 μM–100 μM (B) **[^{3}H] 2_2Br** for 10 (A) or 5 (B) min at 37 °C at pH 5.5. Radioactivity was measured by a Wallac Liquid Scintillator Counter. **C.** Uptake of **[^{3}H] 2_2Br** was measured in the presence or absence of 20 μM BSP (bromosulfophthalein) for 10 min at 37 °C or 0 °C at pH 5.5. B) and C) signal measured in on mock cells were subtracted from that measured in A431-OATP2B1 cells. Data points show the average ± SD values obtained in three independent replicates. Statistical analysis was performed with unpaired t-test (**$p < 0.01$ and ***$p < 0.001$).

increases. Using a single chemical entity with multiple targets is a better strategy to avoid side effects (Meena et al., 2015). Multi-targeted drug design has not only been applied for anti-cancer treatment, but also for inflammatory conditions, Alzheimer's disease and neurodegenerative disorders, as well (Geldenhuys and Van der Schyf, 2013).

Here we identified 2-halogenated-13α-estrones as (potential) OATP2B1 substrates. Since these compounds are also effective HSD1 inhibitors, their increased uptake mediated by OATP2B1 can potentially be exploited to achieve an enhanced anti-tumor effect in estrogen dependent tumors. Though further experiments on estrogen-dependent cell lines expressing the potential targets of 13α-estrones, the STS and/or HSD1 enzymes (e.g. T47D, MCF-7) with and without OATP2B1 overexpression would be needed to clarify this issue.

Author contribution statement

R. L.-R.: performed experiments, analyzed data, wrote manuscript draft, É. B.: performed experiments, analyzed data, wrote manuscript file, R. J.: synthesized purified and quality checked the steroids, Cs. T: synthesized tritiated steroids, wrote the manuscript, E. M.: designed and synthesized the steroids, wrote the manuscript, Cs. Ö-L.: conceptualized the work, analyzed data, wrote the manuscript.

Declaration of Competing Interest

The authors declare that they have no known competing financial interests or personal relationships that could have appeared to influence the work reported in this paper.

Acknowledgements

This work was supported by National Research, Development and Innovation Office-NKFIH through projects [OTKA SNN 124329 (E. M.) and OTKA FK 128751 (Cs. Ö-L.)]. The sponsors had no influence on the design of the experiments, on the interpretation of the data or on the publication.

Appendix A. Supplementary data

Supplementary data to this article can be found online at https://doi.org/10.1016/j.taap.2021.115704.

References

Arakawa, H., Nakanishi, T., Yanagihara, C., Nishimoto, T., Wakayama, T., Mizokami, A., Namiki, M., Kawai, K., Tamai, I., 2012. Enhanced expression of organic anion transporting polypeptides (OATPs) in androgen receptor-positive prostate cancer cells: possible role of OATP1A2 in adaptive cell growth under androgen-depleted conditions. Biochem. Pharmacol. 84, 1070–1077.

Ayan, D., Roy, J., Maltais, R., Poirier, D., 2011. Impact of estradiol structural modifications (18-methyl and/or 17-hydroxy inversion of configuration) on the in vitro and in vivo estrogenic activity. J. Steroid Biochem. Mol. Biol. 127, 324–330.

Bacsa, I., Jojart, R., Schneider, G., Wolfling, J., Maroti, P., Herman, B.E., Szecsi, M., Mernyak, E., 2015. Synthesis of A-ring halogenated 13alpha-estrone derivatives as potential 17beta-HSD1 inhibitors. Steroids 104, 230–236.

Bacsa, I., Herman, B.E., Jojart, R., Herman, K.S., Wolfling, J., Schneider, G., Varga, M., Tomboly, C., Rizner, T.L., Szecsi, M., Mernyak, E., 2018. Synthesis and structure-activity relationships of 2- and/or 4-halogenated 13beta- and 13alpha-estrone derivatives as enzyme inhibitors of estrogen biosynthesis. J. Enzym. Inhib. Med. Chem. 33, 1271–1282.

Bauer, M., Matsuda, A., Wulkersdorfer, B., Philippe, C., Traxl, A., Ozvegy-Laczka, C., Stanek, J., Nics, L., Klebermass, E.M., Poschner, S., Jager, W., Patik, I., Bakos, E., Szakacs, G., Wadsak, W., Hacker, M., Zeitlinger, M., Langer, O., 2018. Influence of

OATPs on hepatic disposition of erlotinib measured with positron emission tomography. Clin. Pharmacol. Ther. 104, 139–147.
Berenyi, A., Minorics, R., Ivanyi, Z., Ocsovszki, I., Ducza, E., Thole, H., Messinger, J., Wolfling, J., Motyan, G., Mernyak, E., Frank, E., Schneider, G., Zupko, I., 2013. Synthesis and investigation of the anticancer effects of estrone-16-oxime ethers in vitro. Steroids 78, 69–78.
Blomquist, C.H., Lindemann, N.J., Hakanson, E.Y., 1984. Inhibition of 17 beta-hydroxysteroid dehydrogenase (17 beta-HSD) activities of human placenta by steroids and non-steroidal hormone agonists and antagonists. Steroids 43, 571–586.
Blomquist, C.H., Leung, B.S., Beaudoin, C., Poirier, D., Tremblay, Y., 1997. Intracellular regulation of 17 beta-hydroxysteroid dehydrogenase type 2 catalytic activity in A431 cells. J. Endocrinol. 153, 453–464.
Buxhofer-Ausch, V., Secky, L., Wlcek, K., Svoboda, M., Kounnis, V., Briasoulis, E., Tzakos, A.G., Jaeger, W., Thalhammer, T., 2013. Tumor-specific expression of organic anion-transporting polypeptides: transporters as novel targets for cancer therapy. J. Drug Deliv. 2013, 863539.
Chen, H., Pan, J., Zhang, L., Chen, L., Qi, H., Zhong, M., Shi, X., Du, J., Li, Q., 2018. Downregulation of estrogen-related receptor alpha inhibits human cutaneous squamous cell carcinoma cell proliferation and migration by regulating EMT via fibronectin and STAT3 signaling pathways. Eur. J. Pharmacol. 825, 133–142.
Durmus, S., van Hoppe, S., Schinkel, A.H., 2016. The impact of Organic Anion-Transporting Polypeptides (OATPs) on disposition and toxicity of antitumor drugs: insights from knockout and humanized mice. Drug Resist. Updat. 27, 72–88.
Fahrmayr, C., Konig, J., Auge, D., Mieth, M., Fromm, M.F., 2012. Identification of drugs and drug metabolites as substrates of multidrug resistance protein 2 (MRP2) using triple-transfected MDCK-OATP1B1-UGT1A1-MRP2 cells. Br. J. Pharmacol. 165, 1836–1847.
Fujita, D., Saito, Y., Nakanishi, T., Tamai, I., 2016. Organic anion transporting polypeptide (OATP)2B1 contributes to gastrointestinal toxicity of anticancer drug SN-38, active metabolite of Irinotecan hydrochloride. Drug Metab. Dispos. 44, 1–7.
Geldenhuys, W.J., Van der Schyf, C.J., 2013. Designing drugs with multi-target activity: the next step in the treatment of neurodegenerative disorders. Expert Opin. Drug Discovery 8, 115–129.
Gupta, A., Kumar, B.S., Negi, A.S., 2013. Current status on development of steroids as anticancer agents. J. Steroid Biochem. Mol. Biol. 137, 242–270.
Hagenbuch, B., Stieger, B., 2013. The SLCO (former SLC21) superfamily of transporters. Mol. Asp. Med. 34, 396–412.
Hamada, A., Sissung, T., Price, D.K., Danesi, R., Chau, C.H., Sharifi, N., Venzon, D., Maeda, K., Nagao, K., Sparreboom, A., Mitsuya, H., Dahut, W.L., Figg, W.D., 2008. Effect of SLCO1B3 haplotype on testosterone transport and clinical outcome in caucasian patients with androgen-independent prostatic cancer. Clin. Cancer Res. 14, 3312–3318.
Jojart, R., Pecsy, S., Keglevich, G., Szecsi, M., Rigo, R., Ozvegy-Laczka, C., Kecskemeti, G., Mernyak, E., 2018. Pd-Catalyzed microwave-assisted synthesis of phosphonated 13alpha-estrones as potential OATP2B1, 17beta-HSD1 and/or STS inhibitors. Beilstein J. Org. Chem. 14, 2838–2845.
Jojart, R., Ali, H., Horvath, G., Kele, Z., Zupko, I., Mernyak, E., 2020. Pd-catalyzed Suzuki-Miyaura couplings and evaluation of 13alpha-estrone derivatives as potential anticancer agents. Steroids 164, 108731.
Jójárt, R., Laczkó-Rigó, R., Klement, M., Kőhl, G., Kecskeméti, G., Özvegy-Laczka, C., Mernyák, E., 2021. Design, synthesis and biological evaluation of novel estrone phosphonates as high affinity organic anion-transporting polypeptide 2B1 (OATP2B1) inhibitors. Bioorg. Chem. 112, 104914.
Konig, J., Cui, Y., Nies, A.T., Keppler, D., 2000. A novel human organic anion transporting polypeptide localized to the basolateral hepatocyte membrane. Am. J. Physiol. Gastrointest. Liver Physiol. 278, G156–G164.
Kovacsics, D., Patik, I., Ozvegy-Laczka, C., 2017. The role of organic anion transporting polypeptides in drug absorption, distribution, excretion and drug-drug interactions. Expert Opin. Drug Metab. Toxicol. 13, 409–424.
Kullak-Ublick, G.A., Ismair, M.G., Stieger, B., Landmann, L., Huber, R., Pizzagalli, F., Fattinger, K., Meier, P.J., Hagenbuch, B., 2001. Organic anion-transporting polypeptide B (OATP-B) and its functional comparison with three other OATPs of human liver. Gastroenterology 120, 525–533.
Laczko-Rigo, R., Jojart, R., Mernyak, E., Bakos, E., Tuerkova, A., Zdrazil, B., Ozvegy-Laczka, C., 2020. Structural dissection of 13-epiestrones based on the interaction with human Organic anion-transporting polypeptide, OATP2B1. J. Steroid Biochem. Mol. Biol. 200, 105652.
Lee, C.I., Goodwin, A., Wilcken, N., 2017. Fulvestrant for hormone-sensitive metastatic breast cancer. Cochrane Database Syst. Rev. 1, CD011093.
Matsumoto, J., Ariyoshi, N., Sakakibara, M., Nakanishi, T., Okubo, Y., Shiina, N., Fujisaki, K., Nagashima, T., Nakatani, Y., Tamai, I., Yamada, H., Takeda, H., Ishii, I., 2015. Organic anion transporting polypeptide 2B1 expression correlates with uptake of estrone-3-sulfate and cell proliferation in estrogen receptor-positive breast cancer cells. Drug Metab. Pharmacokinet 30, 133–141.
Meena, P., Nemaysh, V., Khatri, M., Manral, A., Luthra, P.M., Tiwari, M., 2015. Synthesis, biological evaluation and molecular docking study of novel piperidine and piperazine derivatives as multi-targeted agents to treat Alzheimer's disease. Bioorg. Med. Chem. 23, 1135–1148.
Mostaghel, E.A., Cho, E., Zhang, A., Alyamani, M., Kaipainen, A., Green, S., Marck, B.T., Sharifi, N., Wright, J.L., Gulati, R., True, L.D., Loda, M., Matsumoto, A.M., Tamae, D., Penning, T.N., Balk, S.P., Kantoff, P.W., Nelson, P.S., Taplin, M.E., Montgomery, R.B., 2017. Association of tissue abiraterone levels and SLCO genotype with intraprostatic steroids and pathologic response in men with high-risk localized prostate Cancer. Clin. Cancer Res. 23, 4592–4601.
Nozawa, T., Suzuki, M., Takahashi, K., Yabuuchi, H., Maeda, T., Tsuji, A., Tamai, I., 2004. Involvement of estrone-3-sulfate transporters in proliferation of hormone-dependent breast cancer cells. J. Pharmacol. Exp. Ther. 311, 1032–1037.
Patik, I., Szekely, V., Nemet, O., Szepesi, A., Kucsma, N., Varady, G., Szakacs, G., Bakos, E., Ozvegy-Laczka, C., 2018. Identification of novel cell-impermeant fluorescent substrates for testing the function and drug interaction of Organic Anion-Transporting Polypeptides, OATP1B1/1B3 and 2B1. Sci. Rep. 8, 2630.
Pizzagalli, F., Hagenbuch, B., Stieger, B., Klenk, U., Folkers, G., Meier, P.J., 2002. Identification of a novel human organic anion transporting polypeptide as a high affinity thyroxine transporter. Mol. Endocrinol. 16, 2283–2296.
Rizner, T.L., Thalhammer, T., Ozvegy-Laczka, C., 2017. The importance of steroid uptake and intracrine action in endometrial and ovarian cancers. Front. Pharmacol. 8, 346.
Roth, M., Obaidat, A., Hagenbuch, B., 2012. OATPs, OATs and OCTs: the organic anion and cation transporters of the SLCO and SLC22A gene superfamilies. Br. J. Pharmacol. 165, 1260–1287.
Sang, X., Han, H., Poirier, D., Lin, S.X., 2018. Steroid sulfatase inhibition success and limitation in breast cancer clinical assays: an underlying mechanism. J. Steroid Biochem. Mol. Biol. 183, 80–93.
Schafer, B., Orban, E., Kele, Z., Tomboly, C., 2015. Tritium labelling of a cholesterol amphiphile designed for cell membrane anchoring of proteins. J. Label. Comp. Radiopharm. 58, 7–13.
Schafer, A.M., Bock, T., Meyer Zu Schwabedissen, H.E., 2018. Establishment and validation of competitive counterflow as a method to detect substrates of the organic anion transporting polypeptide 2B1. Mol. Pharm. 15, 5501–5513.
Schonecker, B., Lange, C., Kotteritzsch, M., Gunther, W., Weston, J., Anders, E., Gorls, H., 2000. Conformational design for 13alpha-steroids. J. Organomet. Chem. 65, 5487–5497.
Szabo, J., Jerkovics, N., Schneider, G., Wolfling, J., Bozsity, N., Minorics, R., Zupko, I., Mernyak, E., 2016a. Synthesis and in vitro antiproliferative evaluation of C-13 epimers of triazolyl-d-secoestrone alcohols: the first potent 13alpha-d-secoestrone derivative. Molecules 21.
Szabo, J., Pataki, Z., Wolfling, J., Schneider, G., Bozsity, N., Minorics, R., Zupko, I., Mernyak, E., 2016b. Synthesis and biological evaluation of 13alpha-estrone derivatives as potential antiproliferative agents. Steroids 113, 14–21.
Thakkar, N., Lockhart, A.C., Lee, W., 2015. Role of organic anion-transporting polypeptides (OATPs) in cancer therapy. AAPS J. 17, 535–545.
Van Asten, K., Neven, P., Lintermans, A., Wildiers, H., Paridaens, R., 2014. Aromatase inhibitors in the breast cancer clinic: focus on exemestane. Endocr. Relat. Cancer 21, R31–R49.
Windt, T., Toth, S., Patik, I., Sessler, J., Kucsma, N., Szepesi, A., Zdrazil, B., Ozvegy-Laczka, C., Szakacs, G., 2019. Identification of anticancer OATP2B1 substrates by an in vitro triple-fluorescence-based cytotoxicity screen. Arch. Toxicol. 93, 953–964.
Wright, J.L., Kwon, E.M., Ostrander, E.A., Montgomery, R.B., Lin, D.W., Vessella, R., Stanford, J.L., Mostaghel, E.A., 2011. Expression of SLCO transport genes in castration-resistant prostate cancer and impact of genetic variation in SLCO1B3 and SLCO2B1 on prostate cancer outcomes. Cancer Epidemiol. Biomark. Prev. 20, 619–627.
Yaremenko, Feodor G., Khvat, Alexandr V., 1994. A new One-pot synthesis of 17-oxo-13α-steroids of the androstane series from their 13ß-analogues. Mendeleev Commun. 4, 187–188.